Metallomics

Pb(II) binding to the brain specific mammalian metallothionein isoform MT3 and its isolated αMT3 and βMT3 domains

Journal:	*Metallomics*
Manuscript ID	MT-ART-10-2018-000294.R1
Article Type:	Paper
Date Submitted by the Author:	12-Nov-2018
Complete List of Authors:	Perez, Catalina ; Universitat Autònoma de Barcelona, Departament de Química; Universidad de Santiago de Chile, Ciencias de los Materiales Leiva-Presa, Àngels; Universitat de Vic – Universitat Central de Catalunya, Departament de Biociències Austin, Rachel; Barnard College, Chemistry Capdevila, Mercè; Universitat Autònoma de Barcelona, Departament de Química Palacios, Oscar; Universitat Autònoma de Barcelona, Departament de Química

In this work we characterize the binding of a toxic metal ion, as Pb(II), to the brain specific MT3 isoform. This interaction has never been described in the same extension as it has been shown here (speciation by MS, protein folding by CD, thermodynamics by ITC) and the results provide very valuable information to the scientific community that must help to shed light to the relationship between Pb, MT3 and neurodegenerative diseases as Alzheimer or Parkinson's.

Pb(II) binding to the brain specific mammalian metallothionein isoform MT3 and its isolated αMT3 and βMT3 domains

Catalina Pérez-Zúñiga[a§], Àngels Leiva-Presa[b], Rachel Narehood Austin[c], Mercè Capdevila[a], Òscar Palacios[a*]

[a] *Departament de Química, Facultat de Ciències. Universitat Autònoma de Barcelona. .E-08193 Cerdanyola del Vallès, Barcelona, Spain.*
[b] *Aquatic Ecology Group, Departament de Biociències, Facultat de Ciències i Tecnologia, Universitat de Vic – Universitat Central de Catalunya, E-08500 Vic, Barcelona, Spain*
[c] *Department of Chemistry, Barnard College, Columbia University, NY, NY 10027, USA*

* Corresponding author: Oscar.palacios@uab.cat
§ Actual address: *Departamento de Química de los Materiales, Facultad de Química y Biología, Universidad de Santiago de Chile. Av. Libertador Bernardo O´Higgins 3363, Estación Central, Santiago.*

Abstract:
The toxicity of lead, one of the most ubiquitous toxic metals, is well known. Some of its pathological effects are related to its preference for the sulfhydryl groups of proteins. Metallothioneins (MT) are a particular family of metalloproteins characterized by their high Cys content that, among other functions, are linked to the detoxification of heavy metals. In mammals, 4 MT isoforms have been found. The MT3 isoform, also called "neuronal growth inhibitory factor", is mainly synthesized in the brain and contains several structural differences that may contribute to important functional differences between it and other MT isoforms. The abilities of recombinant MT3 and its individual αMT3 and βMT3 fragments to bind Pb(II) have been here investigated, under different pH conditions, by means of spectroscopy, mass spectrometry and isothermal titration calorimetry. The results obtained show that the binding of Pb(II) to the intact MT3 protein is relatively unaffected by pH, while the individual domains interact with Pb(II) in a pH-sensitive manner. The mass spectrometry data reveal the evolution with time of the initially formed Pb-MT complexes. In the case of the full length protein, Pb(II) remains bound for a long period of time. With the isolated fragments, the lead is eventually released. The Pb-species formed depend on the amount of Pb(II) present in solution. The thermodynamic data recorded, as measured by ITC, for the replacement of Zn(II) by Pb(II) in reactions with Zn-MT3, Zn-αMT3 and Zn-βMT3 are all similar, and in all cases, the displacement of Zn(II) by Pb(II) is thermodynamically favorable. Zn-replete and Pb-replete MT3 have distinctive circular dichroism spectra, suggestive of structural differences with different metallation status.

Keywords: mammalian metallothionein, brain MT3 isoform, Pb(II) binding, Circular Dichroism, ESI-MS, Isothermal Titration Calorimetry

Introduction

Lead is one of the most ubiquitous toxic metals, present for centuries in a variety of applications. Consequently, lead is one of the largest environmental problems, even though nowadays there is a world-wide effort to reduce its use. Lead is predominantly found in nature in the cationic Pb(II) form. Organometallic alkyl-Pb compounds are also important because of their high toxicity, but typically exposure to these forms is restricted to occupational settings. Lead has no beneficial role in biology. It induces several pathologies in numerous organs. The main cause of lead's toxicity is its preference for the sulfhydryl groups of proteins. Its neurotoxicity and its effects on hemolysis and heme synthesis are well known [1]. Lead interferes with the activity of δ-aminolevulinic acid dehydratase (ALAD) [2, 3], while in the central nervous system (CNS) it interferes with the release of glutamate, among other undesired effects [4, 5]. In the brain, Pb(II) also substitutes for Ca(II), affecting calcium signaling [6] and synaptic plasticity in the hippocampus [7]. Lead exposure may also be associated with the development of neurodegenerative pathologies such as Alzheimer or Parkinson diseases [8, 9, 10, 11, 12]. In addition to other proteins, such as brain PbBP [13], metallothioneins could play a role in lead detoxification in neurons and glial cells [14, 15].

Metallothioneins (MTs) constitute a large family of ubiquitous metal-binding proteins, able to complex large amounts of diverse metal ions due to their extremely high cysteine (Cys) content [16, 17]. Mammalian MTs consist in four isoforms (MT1 to MT4). All of them have 20 Cys residues, but they have particular

differences in their amino acid composition (**Figure 1**) and in their expression pattern: MT1 and MT2 are synthesized in all tissues, MT3 is mainly synthesized in the brain, and MT4 is only synthesized in skin. All these MTs are assumed to be constituted by two domains, the C-terminal fragment, denominated the α-domain, and the N-terminal part, known as the β-domain.

```
MT1     MDPN-CSCSTGGSCTCTSSCACKNCKCTSCKKSCCSCCPVGCSKCAQGCVCK------GAADKCTCCA
MT2     MDPN-CSCASDGSCSCAGACKCKQCKCTSCKKSCCSCCPVGCAKCSQGCICK------EASDKCSCCA
MT3     MDPETCPCPTGGSCTCSDKCKCKGCKCTNCKKSCCSCCPAGCEKCAKDCVCKGEEGAKAEAEKCSCCQ
MT4     MDPRECVCMSGGICMCGDNCKCTTCNCKTCRKSCCPCCPPGCAKCARGCICKGG------SDKCSCCP
        ***. *.* ..*.*.* * *.*. *.*..*.****.***.**.**...*.**.        ..**.**.
```

Figure 1. Primary structure of mouse MT1, MT2 and MT3 and human MT4. For MT3, blue residues mark the primary structure of αMT3 and red residues mark that of βMT3. *indicates similarity in all amino-acid sequences, and · indicates similarity at least in two amino-acid sequences.

The MT3 isoform, also called “neuronal growth inhibitory factor” (GIF) was found by Uchida and coworkers in 1991 [18] during their studies on Alzheimer’s disease (AD). Since its discovery, researchers have underlined several structural differences that may contribute to important functional differences between MT3 and MT1 or MT2, which are the best known mammalian MT isoforms. Indeed, with 20 Cys residues (9 in the β domain and 11 in its α domain) in a total of 68 residues, MT3 is the unique mammalian MT isoform to possess 2 prolines in its β domain and an acid hexapeptide loop in the α domain [19]. Unlike most MTs, MT3 is not induced by metal ions [20]. Its intra- and extracellular functions appear to include, among others, the inhibition of neuronal growth, maintaining Zn(II) and Cu(I) homeostasis in astrocytes and neurons, contributing to the use of Zn(II) as a neuromodulator, and protection against reactive oxygen and nitrogen species [21] or free Cu(II) ions [22]. However, the biological significance of metal binding to MT3 still remains to be determined.

Even if MT1, MT2 and MT3 are present in the brain of mammals, each MT isoform may function differently, indicating a multifunctional role over a wide range of cellular processes. MT3 is mainly found in neurons, and preliminary reports suggest that it is involved in the control of amyloid plaque aggregation proteins or *α*-synuclein, related with neurodegenerative disorders such as Alzheimer's and Parkinson's diseases [14, 15].

As isolated, MTs are bound to the endogenous metal ions Zn(II) and/or Cu(I) [23]. Metal-MTs affinities follow the inorganic scale of affinity of metal ions for thiolates: Hg(II) > Ag(I) ~ Au(I) > Cu(I) > Cd(II) > Pb(II) > Co(II) ~ Zn(II) ~ Fe(II) [24]. Thus, it should be possible to substitute the Zn(II) bound to an MT by any other metal ion with higher affinity. This has been widely studied in the literature [25, 26, 27, 28, 29, 30, 31]: the binding of Zn(II) and Cu(I) in recombinant expression system [32]; and the *in vitro* binding of Zn(II) and Cd(II) [25, 33, 34]. It was also shown by ^{113}Cd NMR spectroscopy that MT3, similarly to MT1 and MT2, comprises two domains when binding to divalent metal ions, forming two metal–thiolate clusters: M_4S_{11} in the C-terminal α-domain and M_3S_9 in the N-terminal β-domain [35, 36]. The solution structure of the C-terminal domain loaded with Cd(II), Cd_4-αMT3, was reported [37]. This has revealed different backbone flexibilities for each fragment, with the N-terminal residues more flexible. Recent studies, carried out in our research group, have revealed the Cu-thionein character of this special isoform [32]. When purified from living organisms, βMT3 binds 4 molar equivalents of Cu(I) ions while αMT3 binds 3 molar equivalents of Zn(II) ions [38]. Unlike βMT3, which possesses greater stability, αMT3 is sensitive to air oxidation [39]. MTs are consequently proposed to function in heavy metal detoxification as they sequester Cd(II) and Hg(II) by replacing Zn(II) metal ions [40, 41].

As another toxic thiophilic exogenous metal ion, interactions of Pb(II) with MTs have already been reported [42, 43, 44, 45, 46, 47]. However, many questions about the structure and composition of the Pb-MTs complexes remain still unanswered. What is the structure of Pb(II) bound to MT3? How many Pb(II) ions bind to the protein? Is the binding of lead to the intact protein mirrored by the binding of lead to each subunit as is thought to be the case with other metal ions or is there some sort of cooperativity in the intact protein? Pb(II) is an intermediate Lewis acid, able to form compounds with a wide range of coordination numbers (from 2 to 12) and a wide number of possible coordination geometries. The low solubility of the $Pb(OH)_2$ species (several solubility products were found in the literature, from 10^{-15} to 10^{-20}) that is formed at pH > 6, as well as the formation of a wide set of cationic species, $Pb_x(OH)_y^{n+}$ (x, y =1-4) are also well known. Their formation depends on pH, the concentration of Pb(II) and the ionic strength [48, 49]. The presence of chloride anions that easily form insoluble $PbCl_2$, makes it difficult to predict the interaction of Pb(II) with

chelating species, such as MTs. An earlier report of Pb binding to other MTs [44] suggests that lead may have intriguing temporal chemistry when it interacts with MTs.

Lead's differential binding to zinc sites in proteins are thought to contribute to its toxicity. MT3's effects in the brain may rely on protein-protein interactions where protein shape is critical [50]. Literature provides compelling evidences to think that Pb(II) and MT3 do interact in brain [51], and in fact exposure to low levels of lead in young rats increases MT3 expression [52]. Therefore it is important to study whether lead does displace Zn(II) from MT3 and if MT3 changes shape when lead displaces zinc. In this work, we focus on the coordination of Pb(II) to the recombinantly synthesized mouse MT3, as well as to each of its isolated domains, αMT3 and βMT3, at different pH values and in the absence of Cl^- ions. Metal binding features have been studied by means of spectroscopic techniques, mainly circular dichroism (CD) and UV-visible absorption, as well as electrospray ionization mass spectrometry (ESI-MS). Moreover, thermodynamic data for the coordination of Pb(II) to the three proteins was determined by isothermal titration calorimetry (ITC).

Experimental Section

Recombinant synthesis, purification and characterization of the Zn-MT3 complexes

The MT3-GST, αMT3-GST and βMT3-GST fusion polypeptides were biosynthesized as previously reported by our group [32]. Expression was induced with isopropyl β-D-thiogalactopyranoside (IPTG) and cultures were supplemented with 300 μM $ZnCl_2$, final concentrations, to form the Zn-MT species. Total protein extract was prepared from these cells as previously described [53]. Metal complexes were recovered from the MT3-GST, αMT3-GST and βMT3-GST fusion constructs by thrombin cleavage and batch-affinity chromatography using Glutathione-Sepharose 4B (General Electric HC). After concentration using Centriprep Microcon 3 (Amicon), metal complexes were finally purified by FPLC in a Superdex75 column (General Electric HC) equilibrated with 50 mM Tris-$HClO_4$, pH 7.5. The samples were kept at -80 ºC until use. All procedures were performed using argon (pure grade 5.0) saturated buffers, and all syntheses were performed at least twice to ensure reproducibility.

The S and the Zn content of each preparation was determined by means of inductively coupled plasma atomic emission spectroscopy (ICP-AES) in a Polyscan 61E (Thermo Jarrell Ash) spectrometer, measuring S at 182.040 nm and Zn at 213.856 nm. The concentration of each protein and the Zn-to-protein ratios (Zn/MT) were calculated from the S and Zn content of the samples, taking into account the number of cysteine and methionine residues present in each peptide.

In vitro Pb-binding studies of MT3, αMT3 and βMT3

The titrations of the Zn-MT preparations with Pb(II) at pH 4.5 and 7.0 were carried out following the methodology previously described [53, 54], using a standardized $Pb(ClO_4)_2$ solution (pH 4.5). A Jasco spectropolarimeter (Model J-715) interfaced to a computer (J700 software) was used for CD measurements at a constant temperature (25 or 55 ºC) maintained by a Peltier PTC-351S apparatus. Electronic absorption measurements were performed on an HP-8453 Diode array UV-visible spectrophotometer. All spectra were recorded with 1-cm capped quartz cuvettes, corrected for the dilution effects and processed using the GRAMS 32 program.

CD and UV-visible spectra were recorded at the different experimental conditions, both always immediately after Pb(II) addition and each subsequent 10 minutes until no change was detected in consequent spectra. When necessary, difference UV-visible spectra were represented in order to better analyze the evolution from two consecutive Pb(II) molar equivalent additions. The addition of "*x* molar equivalents of Pb(II)" is denoted below as "*x* Pb(II) eq". During all experiments, strict oxygen-free conditions were kept by saturation of all the solutions with argon. In the experiments at acidic pH, the initial solutions buffered with Tris-$HClO_4$ at neutral pH were lowered to pH 4.5 by addition of $HClO_4$.

Electrospray ionization mass spectrometry analyses of the metal-MT complexes

Molecular weight (MW) determinations were performed by electrospray ionization time-of-flight mass spectrometry (ESI-TOF MS) on a Micro Tof-Q instrument (Bruker) interfaced with a Series 1200 HPLC Agilent pump, equipped with an autosampler, all of which were controlled by the Compass Software. Calibration was attained with 0.2 g NaI dissolved in 100 mL of a 1:1 H_2O:isopropanol mixture. Samples containing MT complexes were analyzed at 40 μL min^{-1} flow rate, in a spectra collection range 800-2500 m/z. The carrier buffer was a 5:95 mixture of acetonitrile:ammonium acetate/ammonia (15 mM, pH 7.0).

Determination of thermodynamic constants by isothermal titration calorimetry

ITC experiments were performed with a Microcal VP-ITC (Northampton, MA, USA) at 25°C and pH 4.5. The reference solution contained 50 mM Tris-$HClO_4$ at pH 4.5. Samples of Zn-αMT3, Zn-βMT3 and Zn-MT3 contained 50 mM Tris-$HClO_4$ and 20 μM, 20 μM and 10 μM of protein, respectively. The $Pb(ClO_4)_2$ titration solution contained sufficient Pb(II) ions, in Tris-$HClO_4$ 50 mM, to provide the Pb(II) equivalents required for each experiment. The pH of all the solutions used was decreased to 4.5 by addition of $HClO_4$ acid. The injection were made normally each 5 minutes until signal stabilization was observed. Apparent equilibrium constants, metal stoichiometry, and changes in enthalpy and entropy were estimated from the resulting titration curves using equivalents site model in the Origin analysis software. The software uses a nonlinear least-squares algorithm and the concentrations of the titrant and the sample to fit the heat developed or consumed in each injection to an equilibrium binding equation. The results considered correspond to the average of, at least, two independent experiments under the same experimental conditions and in different days. The different fitting available in the software were applied to the data until reaching the one with lowest error associated. The errors associated with the experimental data are indicated together with in the experimental values.

Results and Discussion

Characterization of the Zn-MT3, Zn-αMT3 and Zn-βMT3 preparations

The recombinant proteins here used were produced as following established procedures from the laboratory of Silvia Atrian's group [32, 53]. In this case, the amino acid sequences were obtained from the cDNA of mouse MT3 (UniProtKB/Swiss-Prot,accession number P28184) and produced as GST-fusion proteins. As a consequence of the cloning requirements, after purification, the dipeptide Gly-Ser was present at the N-terminus of all polypeptides; however, this had previously been shown not to alter the MT metal-binding capacities [53].

After recombinant production of MT3, αMT3 and βMT3 in Zn(II)-enriched media and further purification, the resulting Zn(II)-proteins were fully characterized by conventional techniques (see experimental section). These proteins were kept in 50 mM Tris-$HClO_4$ to avoid the presence of chloride ions, which would promote precipitation of $PbCl_2$. The results of the initial characterization of the three proteins are shown in **Table 1**.

Protein	[MT] (M)	Zn/MT ratio	ESI-MS
MT3	$2.31\ 10^{-4}$	6.6	$Zn_7 > Zn_6 > Zn_5$
αMT3	$2.32\ 10^{-4}$	4.5	Zn_4
βMT3	$1.72\ 10^{-4}$	3.1	$Zn_3 >> Zn_2$

Table 1. Characterization of the Zn-MT3, Zn-αMT3 and Zn-βMT3 recombinant preparations used in this work: concentration of protein, Zn-to-MT ratios (determined from ICP-AES measurements), and species identified in the ESI-MS spectra at pH 7.0. The CD and MS spectra were equivalent to those reported in reference 32.

The ESI-MS results obtained at neutral pH allowed the identification of several Zn-loaded species in the whole MT3: Zn_7-, Zn_6- and Zn_5-MT3, while practically unique Zn-complexes were observed in the isolated fragments: Zn_4-αMT3 and Zn_3-βMT3. The CD spectra [32] renders low intensity signals at *ca*. 240 nm characteristic of Zn-MT preparations with poorly folded species [23], as expected by their mainly nature as Cu-thioneins [32].

Interaction of Pb(II) with MT3, αMT3 and βMT3

In order to determine the binding abilities of MT3 and its isolated fragments in the presence of Pb(II), different amounts of $Pb(ClO_4)_2$ were added to the corresponding Zn-MT preparations at different experimental conditions. These experiments were monitored by CD, UV-vis and ESI-MS. Titrations were carried out at two different pH values (4.5 and 7.0) in order to see the possible effect of $Pb(OH)_2$ precipitation. The value of pH 4.5 was chosen because at this pH some Zn(II) will still be bound to the protein, but concerns about lead insolubility are minimal.

Prior mass spectrometry work has shown that Pb-MT species evolve with time [44]. This alerted us to the fact that we would need to observe the results of Pb(II) additions to MTs both initially and after time has elapsed, which is different from what we have done with other metal ions [23]. These prior experiments also indicated that the metal-complexes formed and their temporal stability were strongly dependent on the amount of Pb(II) present in the solution.

We therefore followed the ESI-MS temporal evolution of the addition of two selected amounts of Pb(II) at neutral pH and at room temperature: (A) that corresponding to the Pb(II) saturation point of the protein, detected through the spectroscopic data (CD and UV-vis) (7, 4 and 3 Pb(II) eq for MT3, αMT3, and βMT3, respectively), and (B) a high excess of Pb(II) to guarantee the total saturation of the protein (35, 16 and 12 Pb(II) eq for MT3, αMT3, and βMT3, respectively). Temporal evolution of the species formed in solution (at room temperature) was monitored by recording the mass spectra for up to 20 hours, for MT3, or 12 hours, for αMT3 and βMT3.

Pb(II) binding to the whole MT3

The spectroscopic data recorded at acidic and neutral pH (**Figure 2**) show significant similarities. Even considering the different starting points (at pH 4.5 the partial release of Zn(II) ions can be evidenced from the CD signals at 0 Pb added), the CD spectra evolution during the titration reveals the same trends of MT3 at both pH: long stabilization times after the addition of Pb(II) (more than 1h in most of the cases), very similar CD fingerprints (250(+), 340(-) wide, 370(+) and 405(-) nm), and saturation of the spectral envelopes after the addition of 7 or 8 Pb(II) eq. The UV-vis spectra also indicates saturation of the signal after addition of 7 Pb(II) eq and a wide absorption in the 220-420 nm region. Interestingly, the difference UV-vis spectra present absorptions at 250 and 340 nm from the beginning of both experiments, but at neutral pH new maxima are observed after the addition of 6 Pb(II) eq (260, 320 and 380 nm), thus suggesting the formation of different chromophores than those existing at the early stages of the titration which cannot be reproduced at acidic pH, as previously observed for MT2 [45].

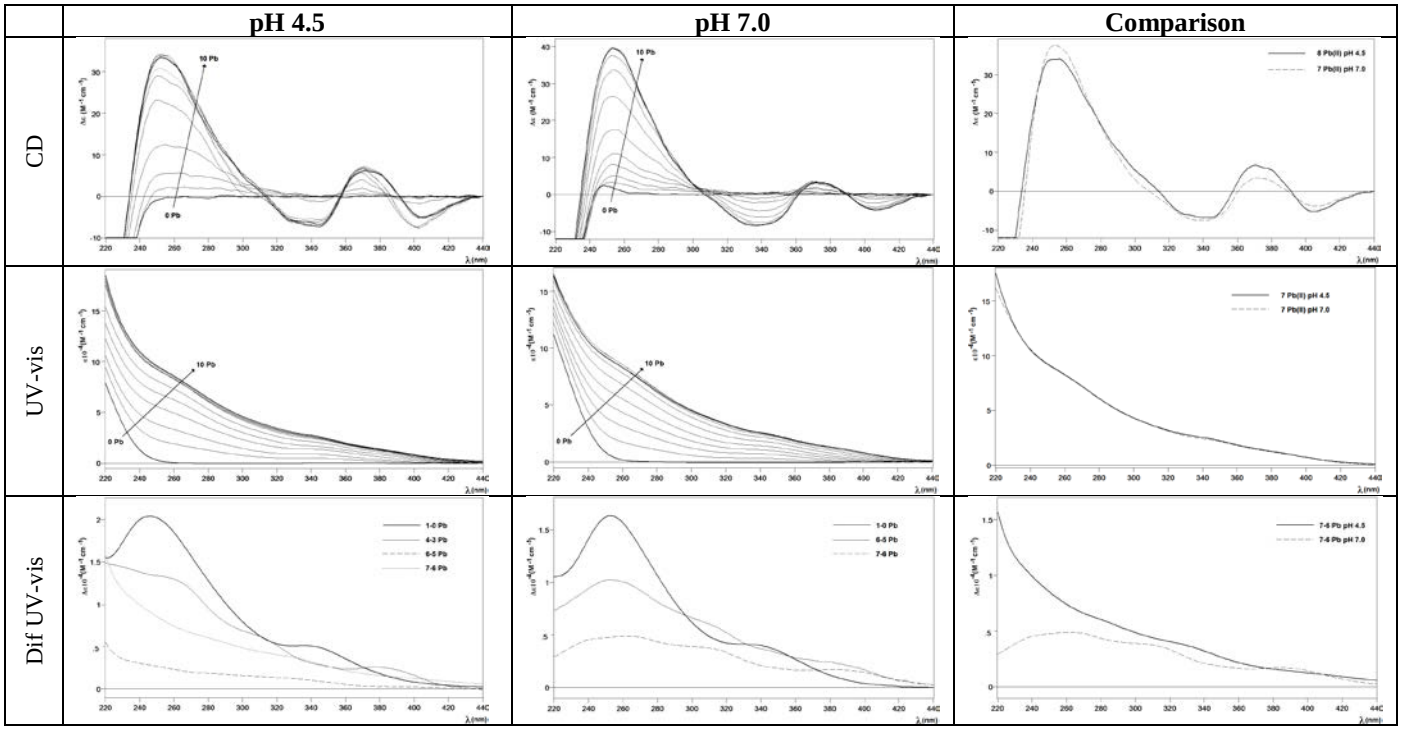

Figure 2. Spectroscopic data (CD, UV-vis and Difference of UV-vis) recorded during the titration of 10 μM solution of Zn-MT3 with $Pb(ClO_4)_2$ at 25 °C and at two pH values: 4.5 and 7.0. The 3rd column shows the spectra corresponding to the same point of the titrations at different pH.

The mass spectra (**Figure 3**) provide information about the coexistence of several metal-complexes throughout the temporal evolution of the two preparations, (A) Zn-MT3 + 7 Pb(II) eq and (B) Zn-MT3 + 35 Pb(II) eq. Aggregates with high Pb(II) content are observed from the beginning of the two additions. Pb_9-MT3 and Pb_{10}-MT3 are the most relevant and abundant species, primarily in the first 4 hours of evolution. During these 4 first hours, no significant alteration of the molecular distribution is observed. After 4 hours, the emergence of heteronuclear Pb_xZn_y-MT3 species (x+y= 7-8) starts to be more evident, especially in the preparation with 7 Pb(II) eq. These complexes increase their abundance with time until 20 hours of evolution. In the last spectra recorded, the main species in the solution with 35 Pb(II) eq are similar to the initially formed, mainly Pb_9-MT3, while in the solution with 7 Pb(II) eq those are the Pb_6Zn_2-MT3 and Pb_5Zn_3-MT3 heteronuclear species.

In general, mass spectrometry data reveal that a mixture of species is always detected at all the stages of the Pb(II) addition experiments. It is notable that the Pb_9- and Pb_{10}-MT3 species were persistently observed in the presence of different amounts of Pb(II), including cases where what would be presumed to be a stoichiometric amount of lead was added. Interestingly, in both experiments the main complexes were loaded with high amounts of Pb(II) and low amounts of Zn(II), suggesting an easy release of the initial Zn(II) ions bound to the protein, probably due to the Cu-thionein character of the MT3 isoform [32].

The data suggest that the binding of Pb(II) to MT3 follows a non-cooperative process, mainly due to the formation of a mixture of several species at the same time, not being possible to observe a single species at any moment. Interestingly, the saturation of the spectroscopic signals after the addition of 7 Pb(II) eq does not confirm the total release of the initial Zn(II) bound to the protein or the formation of a single Pb_7-MT3 species, as already suggested in previous works with other mammalian MT isoforms [55, 56]. This work highlights the importance of combining several techniques when studying the interaction of MTs with non-conventional metal ions, such as Pb(II).

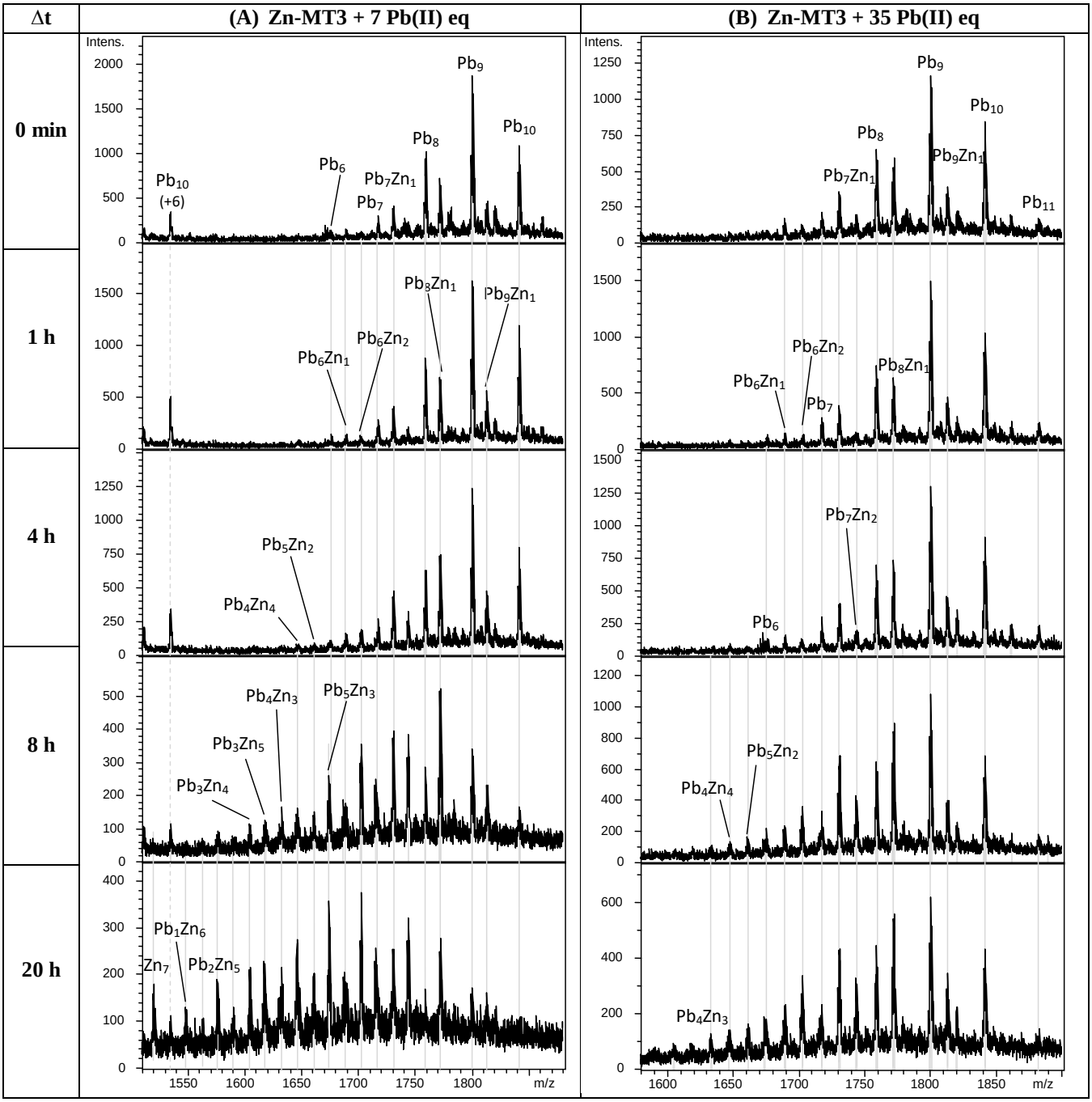

Figure 3. ESI-MS spectra, at the +5 charge state, recorded at pH 7.0 and 25ºC after the addition of (A) 7 Pb(II) eq and (B) 35 Pb(II) eq to 10μM solutions of Zn-MT3. Spectra are recorded after 0 min, 1h, 4h, 8h and 20h after the addition of Pb(II) to the protein solution.

Pb(II) binding to αMT3

The spectroscopic data corresponding to the titration of Zn_4-αMT3 with Pb(II) at acidic and neutral pH conditions are shown in **Figure 4**. In both experiments, 1) stabilization times were shorter than those observed with full length MT3 (10-20 minutes *vs* 1 hour or more) and 2) the addition of 5 Pb(II) eq promotes the saturation of the spectroscopic signals, as previously observed for 7 Pb(II) eq in the entire MT3. The CD data show that, even though similar absorptions are observed in both titrations (at *ca*. 270(-), 300(+), 330(-) and 380(+) nm), the final spectral envelopes are different depending on the pH (as shown in the comparison of the spectra after addition of 5 Pb(II) eq). On the other hand, the same UV-vis features were recorded at both pH values, showing two shoulders (at *ca.* 250 and 340 nm). Accordingly, this result is also confirmed by the UV-vis difference spectra. These features indicate that the Pb(II) coordination geometry in the Pb-αMT3 complexes is independent of the pH of the solution, as the same absorption bands are observed. However, the protein folding about the Pb(II) ions depends on the pH of the media giving similar but not identical clusters at acidic and neutral pH, as indicated by the not superimposable CD envelopes.

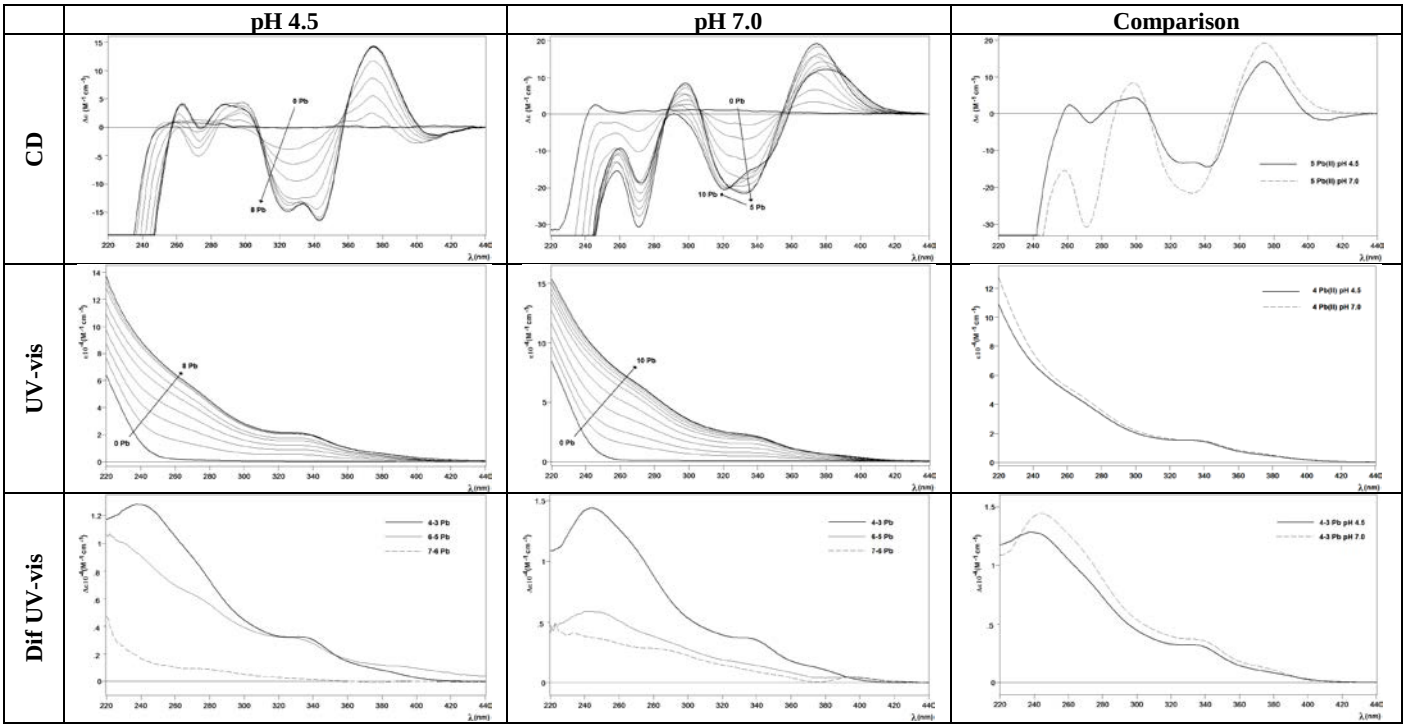

Figure 4. Spectroscopic data (CD, UV-vis and Difference of UV-vis) recorded during the titration of 20 μM solution of Zn_4-αMT3 with $Pb(ClO_4)_2$ at 25 °C and at two pH values: 4.5 and 7.0. The 3rd column shows the spectra corresponding to the same point of the titrations at different pH.

Mass spectra recorded at different times after the addition of 4 (A) and 16 Pb(II) eq (B) to Zn-αMT3 are shown in **Figure 5**.

Data recorded immediately after the addition of 4 Pb(II) eq to Zn_4-αMT3 (denoted as 0 min) (**Figure 5 A**) reveal a partial release of the initial Zn(II) bound and the consequent formation of several heteronuclear (Pb_1Zn_1-, Pb_1Zn_2-, Pb_2Zn_1- and Pb_3Zn_1-αMT3) and homonuclear (Pb_1-, Pb_2-, Pb_3-, Pb_4-αMT3) species. Interestingly, the Zn_1-αMT3 and Zn_4-αMT3 zinc-complexes result to be important species, present at almost all the data recorded during time. All the Pb-species formed (Pb_xZn_y-αMT3 and Pb_z-αMT3) tend to disappear in a short period of time, and 30 min after the Pb(II) addition mainly Zn-complexes are only found. After 6 h, practically the unique detected species is the apo-protein. Similarly, data recorded immediately after the addition of 16 Pb(II) eq (denoted as 0 min) (**Figure 5B**) also reveal the formation of heteronuclear and homonuclear species, mainly the same metal-MT complexes as those formed after the addition of 4 Pb(II) eq, but now, those with higher amounts of Pb(II) are more abundant. Interestingly, the addition of a high excess of Pb(II) released more of the initial Zn(II) than in the previous experiment. The main species formed are shown to be homonuclear (Pb_1-, Pb_2-, Pb_3- and Pb_4-αMT3) and still present in solution after 30 min. The following mass spectra (after 1 h 30 min and 6 h) reveal the total disappearance of all the previous initial species observed previously but the last spectra (recorded at 12 and 24 h after the addition of Pb(II)) showed the presence of Zn_1-αMT3 and Pb_1-αMT3. All these data suggests that the replacement of Zn(II) by Pb(II) in the initial Zn_4-αMT3 protein occurs rapidly and that mainly Pb(II) homonuclear complexes are formed. Additionally, even if the species formed are practically the same after the addition of different amounts of Pb(II), it is also clear that the formation of the species containing higher Pb(II) amounts require an important excess of this metal in solution. In both cases, the Pb-containing complexes initially formed disappear with time, giving rise to the formation of species with lower metal content (apo-αMT3 in the case of 4 Pb(II) eq added and also Zn_1-αMT3 in presence of excess of Pb(II)). Consequently, under the assayed ESI-MS conditions, Pb-αMT3 species are not stable enough at neutral or slightly acidic pH to last over time. The reappearance of Zn_1- and Pb_1-αMT3 after a long period of incubation suggest the presence of a secondary process, which promotes the release of Pb(II) ions from MT, or alternatively the formation of ESI-MS elusive species.

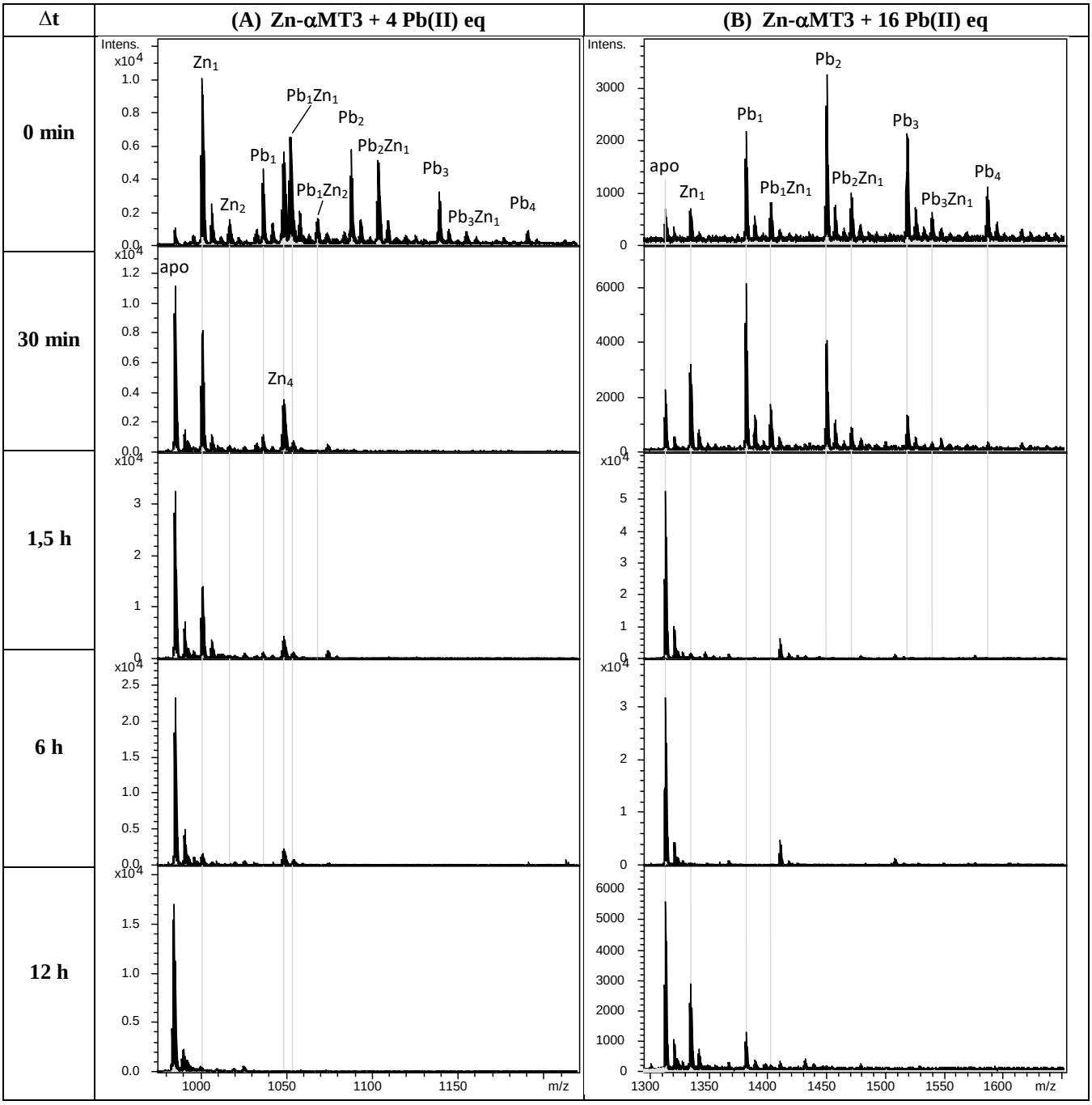

Figure 5. ESI-MS spectra recorded at pH 7.0 and 25ºC after the addition of (A) 4 Pb(II) eq -at the +4 charge state- and (B) 16 Pb(II) eq -at the +3 charge state- to 20μM solutions of Zn_4-αMT3. Spectra are recorded after 0 min, 30 min, 1 h 30 min, 6 h, and 12 h after the addition of Pb(II) to the protein solution. The spectra recorded after 24 h coincide with those recorded after 12 h.

Pb(II) binding to βMT3

The spectroscopic data corresponding to the titration of Zn_3-βMT3 with Pb(II) at acidic and neutral pH conditions are shown in **Figure 6**. The set of CD spectra recorded at acidic pH exhibits increasing CD maxima at 245, 280 and 320 nm until the addition of 5 Pb(II) eq. At neutral pH, the CD fingerprints show also only positive bands at 245, 300, 330 and 370 nm. Saturation of the spectroscopic signals occurs after the addition of 5 and 4 Pb(II) eq, respectively. This saturation point has been observed for 7-8 Pb(II) eq in the entire MT3 and 5 Pb(II) eq for the αMT3, independently of the pH. While at neutral pH the initial CD profile has an unusual positive band at *ca.* 225 nm, attributable to the peptide folding, together with the expected Zn-SCys absorption at 245 nm, at pH 4.5 the CD spectrum resembles those recorded for the apo-MT, suggesting the total release of Zn(II) of the peptide. UV-vis spectra of both titrations are similar, showing two shoulders (at *ca.* 250 and 330-340 nm), but comparison of the UV-vis spectra of the saturation points exhibits a small blue shift of the maxima in the case of the acidic titration, indicating an unequal coordination geometry of Pb(II) at different pH values. These results are confirmed by the UV-vis difference spectra. Thus, unlike the

entire MT3 or the αMT3 fragment, pH seems to influence the folding of the βMT3 peptide with Pb(II) and the coordination geometry of the Pb(II) bound. This observation is consistent with known characteristics of the βMT3 fragment [32].

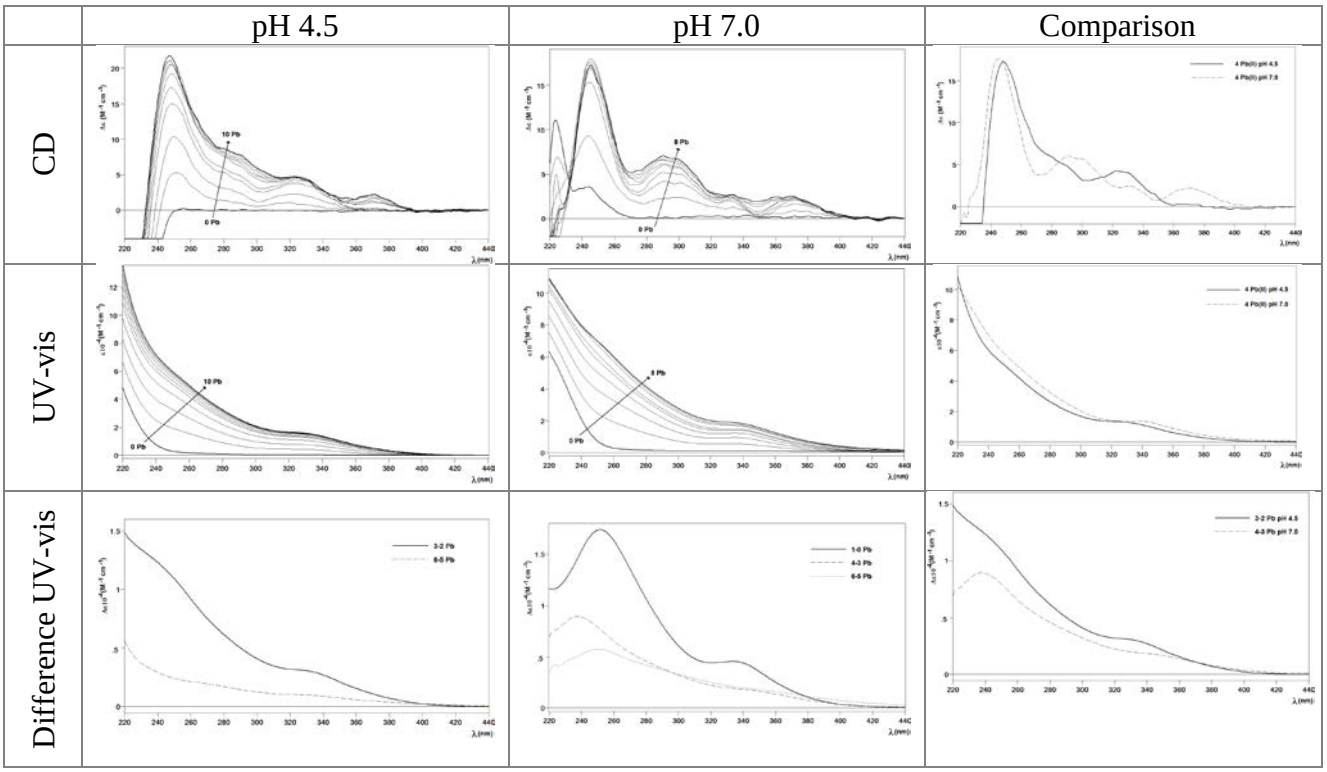

Figure 6. Spectroscopic data (CD, UV-vis and Difference of UV-vis) recorded during the titration of 20 μM solution of Zn_3-βMT3 with $Pb(ClO_4)_2$ at 25 °C and at two pH values: 4.5 and 7.0. The 3rd column shows the spectra corresponding to the same point of the titrations at different pH values.

Mass spectra recorded after the addition of 3 Pb(II) eq (**Figure 7A**) show an immediate formation of a major Pb_1Zn_1-βMT3 heteronuclear species coexisting with Pb_1-, Pb_2-, Pb_2Zn_1-, Pb_3-βMT3, as well as Zn_1-, Zn_2-, and Zn_3-βMT3 as minor complexes. As already observed in the αMT3 fragment, the species with the highest Pb(II) content tend to disappear with time, as revealed by the spectra recorded after 30 min. But 1h 30 min after the addition of $Pb(ClO_4)_2$ to Zn_3-βMT3, practically only Zn_1-βMT3 is detected, while all the previously detected Pb-species are almost absent, and the apo-form becomes more important. Surprisingly, the addition of a high excess of Pb(II) (12 Pb(II) eq) (**Figure 7B**) promotes the formation of major Pb_3-βMT3 and Pb_4-βMT3. There is no evidence of appreciable amounts of any heteronuclear Pb_xZn_y-βMT3 species. Although the same mass spectrum is recorded after 30 min, these species disappear after 1h 30 min of the addition, and only apo-βMT3 was detected in the next spectra. Consequently, an analogous evolution with time of the molecular distribution of the metal-MT species was observed in both experiments: 1) the quick binding of Pb(II) to the βMT3 protein (as already observed both with the MT3 and αMT3 proteins), 2) an initial speciation dependent on the quantity of Pb(II) added to the protein solution (also observed with the MT3 and αMT3 proteins), and 3) the disappearance of Pb-containing species to rendeer the apo-protein (also detected for αMT3 proteins) after 30 min.

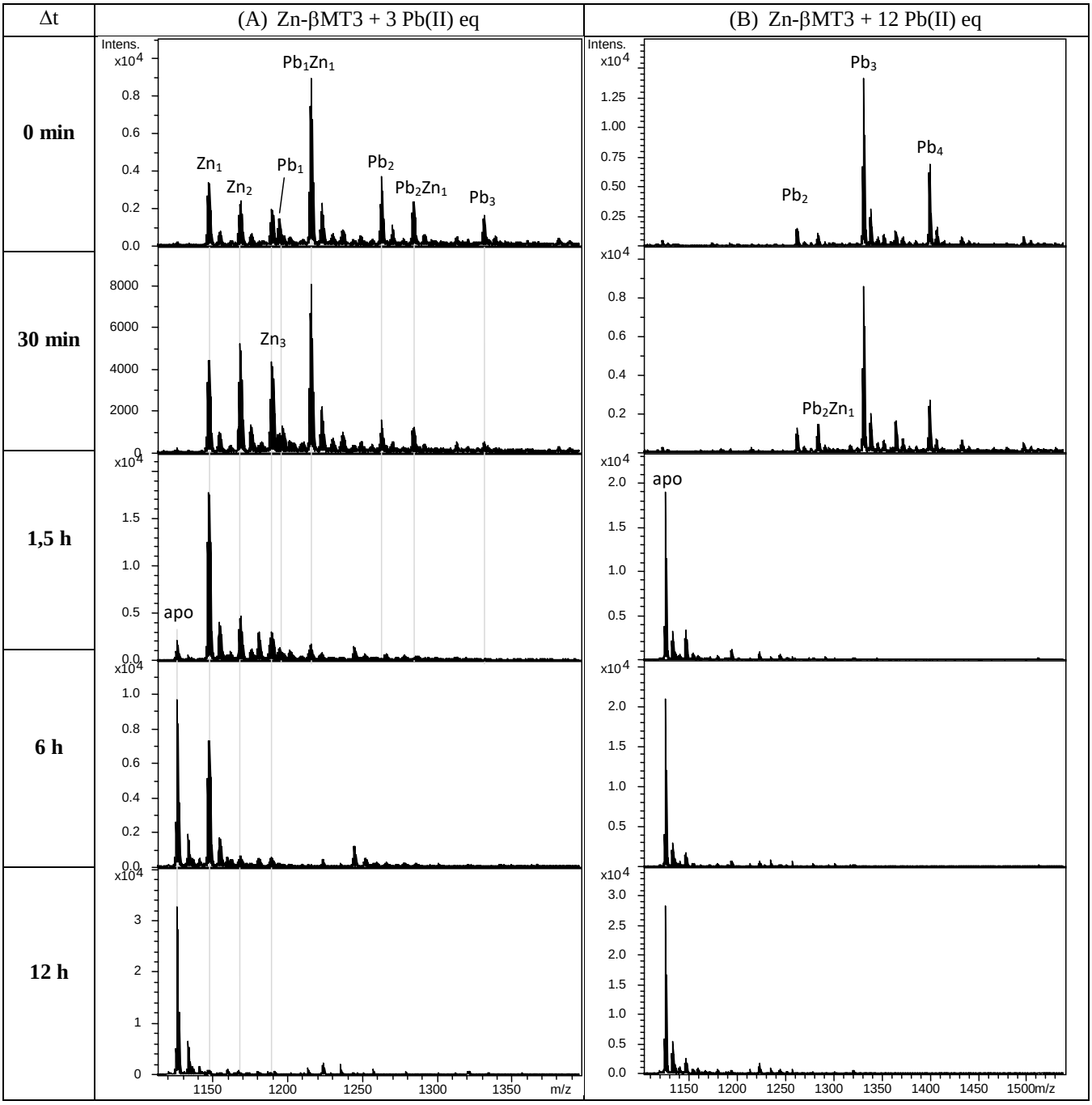

Figure 7. ESI-MS spectra recorded at pH 7.0 and 25ºC after the addition of (A) 3 Pb(II) eq and (B) 12 Pb(II) eq to 20μM solutions of Zn_3-βMT3. Spectra are recorded after 0 min, 30 min, 1h 30 min, 6h, and 12h after the addition of Pb(II) to the protein solution. The spectra recorded after 24 h are exactly to those recorded after 12 h.

When comparing the results obtained for both isolated domains (α and β) some interesting differences deserve to be highlighted. The CD spectra recorded for the Pb-βMT3 species show only-positive bands of lower intensity than those of Pb-αMT3, suggesting that the Pb-αMT3 species exhibit higher chirality than the Pb-βMT3 complexes and thus, probably, the former gives rise to Pb-MT complexes with a better defined 3D structure. In the same way, the maxima observed in the difference UV-vis spectra for βMT3 after Pb(II) addition are mainly two, slightly different from those observed for the αMT3 fragment, where up to 4 different maxima were detected. Finally, the higher stability of the initial Zn-αMT3 species, in regards to that of the βMT3 domain, is reflected by the presence of heteronuclear PbZn-αMT3 after the addition of Pb(II), while analogous heteronuclear complexes are not as important in the case of the βMT3 fragment, especially in the presence of high amounts of Pb(II).

Comparison between αMT3, βMT3 and entire MT3 when binding Pb(II)

The results on the interaction of Pb(II) with recombinant mouse MT3, and with its independent α and β domains, shed light on the putative effect of the pH on the binding abilities of these proteins as well as on

their speciation in the presence of Pb(II). The complexity depicted from the MS data, and especially the coexistence of several metal-complexes that evolve with time, makes difficult the comparison of the whole set of data.

In order to investigate whether the MT3 domains react with Pb(II) in a dependent or independent way, the CD spectra of Pb-αMT3 and Pb-βMT3 were compared with those of Pb-MT3 (**Figure 8**). Only the CD spectra corresponding to the addition of 4 and of 7 Pb(II) eq to Zn-MT3 were taken into account as they respectively represent an intermediate stage and the saturation points observed.

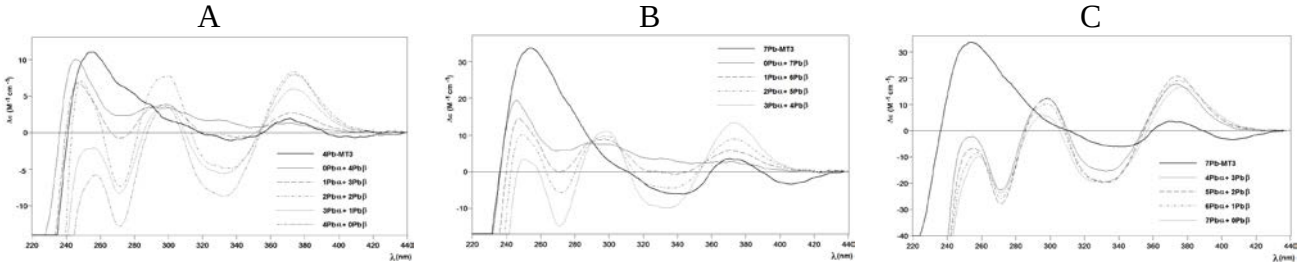

Figure 8. CD spectra corresponding to the addition of (A) 4 and (B and C) 7 Pb(II) eq to Zn_7-MT3 at pH 7.0 and 25 ºC, and addition spectra of the different loading possibilities (same final molar equivalent of Pb(II) added to the α and β isolated domains).

Superimposed spectra show all the distinct possible Pb(II) distributions between domains that satisfy the global stoichiometries formed with 4 and 7 Pb(II) eq added. As can be observed in **Figure 8A**, none of the CD envelopes constructed by summation of two spectra (one of each domain) reproduce that of the entire protein recorded after 4 Pb(II) eq added. A similar scenario can be found when comparing the spectra after addition of 7 P(II) eq (**Figures 8B** and **C**). The folding of the entire MT3 partially resembles the data recorded for 2Pbα+5Pbβ and 3Pbα+4Pbβ (in general, lowPbα+highPbβ, **Figure 8B**) more than those of highPbα+lowPbβ (**Figure 8C**). This finding suggests that probably the binding of the first Pb(II) equivalents to the entire MT3 takes place mainly in the β domain, but not in an independent way because the CD envelopes are not exactly reproduced by the addition of the signals of the individual fragments.

In the comparison of the entire MT3 with its individual domains, it is very important to highlight that while MT3 is able to keep certain amounts of Pb(II) bound for several hours, this is not the case of the isolated domains. This is consistent with the coordination requirements of Pb(II), as it is able to reach different coordination numbers and environments, which probably must require the presence of a longer peptide, rather than small ones, to fulfill its coordination requirements. This is in concordance with the long times needed to get stable CD data in the case of the MT3 protein.

Study of the Pb(II) binding to Zn-MT3, Zn_4-αMT3 and Zn_3-βMT3 by ITC

Isothermal Titration Calorimetry (ITC) was used to determine the thermodynamic parameters associated with the replacement of Zn(II) by Pb(II) by measuring the heat transfer occurring during this reaction. Controlled quantities of $Pb(ClO_4)_2$ were added to solutions of Zn-MT3, Zn-αMT3 and Zn-βMT3, keeping all the solutions used at pH 4.5 in order to avoid precipitation of $Pb(OH)_2$ or the formation of related species [49]. For each Pb(II) addition, the change of heat in the solution (emission of heat in exothermic processes) was measured and the titrations curves (thermograms) represented in **Figure 9** were obtained.

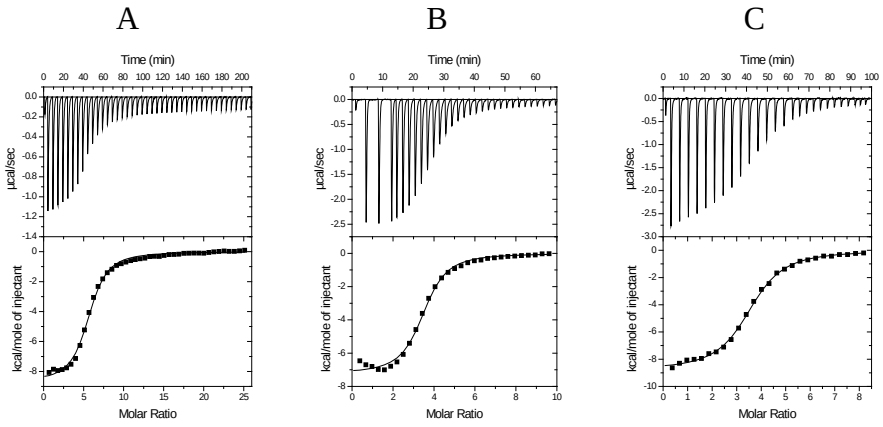

Figure 9. ITC thermograms recorded for the replacement of Zn(II) by Pb(II) in (a) a 10 µM Zn-MT3, (b) 20 µM Zn-αMT3 and (c) 20 µM Zn-βMT3 preparations recorded at pH 4.5 and 25 ºC. The upper panel presents the calorimetric trace, while the bottom panel

shows the integrated heats of injection. The solid line represents the best fit for a one-binding-site model. The two first points were always not considered.

The experimental points were fitted to a model curve that assumed independent binding sites, thus allowing us to obtain the number of binding sites or stoichiometric number (N), and the apparent constant related with the process, Kapp (**Table 2**).

	N	Kapp
MT3	5.6 ± 0.5	4.2 (± 0.4) x 10^5
αMT3	3.4 ± 0.3	5.1 (± 0.6) x 10^5
βMT3	3.5 ± 0.2	3.4 (± 0.2) x 10^5

Table 2. Thermodynamic parameters (stoichiometric number, N, which is molar ratio of metal to protein; and apparent equilibrium constant, Kapp;) for the replacement of Zn(II) by Pb(II) in Zn-MT3, Zn_4-αMT3 and Zn_3-βMT3 at pH 4.5 and 25 ºC. The values here presented correspond to the average of, at least, two independent experiments.

The apparent equilibrium constants (Kapp) represent not only the binding of Pb(II) to the proteins but also the hydration of the leaving Zn^{2+} ions and the necessary dehydration of the Pb^{2+} cations. The hydration energy of gaseous Pb(II) is -1481 kJ mol^{-1} and that of Zn(II) is -2046 kJ mol^{-1} [57], so these differences in aqueous thermodynamics contribute to the overall thermodynamics reported. It must also be considered that at this pH value (4.5) the protein will be partially demetallated and, consequently, protonated cysteines can lose their proteins to bind Pb(II) ions Even if the pH remained constant during all the titration, the possible contribution of deprotonation processes can also affect the Kapp value.

The good fit of the one-binding-site model curves to the experimental points recorded is indicative of the similarity of the available binding sites of the proteins to accommodate Pb(II) ions, although at the beginning of the titrations the theoretical curve is not fitting as well as in the latter stages of the titration. Similar equilibrium constants were obtained for each studied protein (MT3, αMT3 or βMT3), ranging from 3.4 x 10^5 and 5.1 x 10^5, and enthalpy changes (data not shown) were negative in all cases, indicating that the replacement of Zn(II) by Pb(II) in these proteins is, as expected, an exothermic process. However, the number of binding sites for lead are practically identical (about 3.5) for the αMT3 and βMT3 fragments, and similar to those deduced from the spectroscopic data, whereas in the case of the entire MT3 it is 5.6 (± 0.5), lower than the saturation point deduced by spectroscopic techniques, probably due to the partial release of Zn(II) under the assayed conditions.

Our values are very similar to those recently reported values for Pb(II) displacement of Zn(II) to MT2 [43] (5.3 x 10^5 at pH 4.7), and to MT3 (3.1 x 10^5 at pH 6) [47]. The experiments reported with MT3, even if carried out in MES buffer at pH 6, not only showed similar Kapp value to our data with the entire MT3, but also similar saturation parameter was reported (N = 5.8). This confirms the validity of the thermodynamic data here presented and, consequently, support all the conclusions drawn from them.

As expected, the Kapp values here presented for the displacement of Zn(II) bound to MT3 by Pb(II), and related peptides, are very different from the association values reported by Kagi [58] using voltammetry to study the binding of Pb(II) to the apo-form of mammalian MTs (2.5 x 10^{13} at neutral pH). In this case, they determined only the direct binding of Pb(II) to the protein without the requirement of replacing any metal ion previously bound. Even thus, their findings confirmed that the association value for Pb(II) is higher than for Zn(II) at neutral pH (2.5 x 10^{13} *vs.* 5 x 10^{11}) but lower for that of Cd(II) (5 x 10^{15}), as expected when considering the Irving-Williams series. This is again fully consistent with the finding reported in the work here presented.

Conclusion

Our results on the Pb(II) binding abilities of recombinant MT3 and its individual αMT3 and βMT3 fragments provide experimental evidence to support several conclusions. First, the evolution of the CD and electronic absorption spectra during the titration of each fragment of MT3 with Pb(II) show that αMT3 and βMT3 can bind Pb(II) rapidly even at room temperature, despite the long times required for stabilization of the CD signals in the entire MT3 under the same conditions. Only the entire MT3 protein seems to be unaffected by the pH, while the binding abilities of both fragments were shown to be slightly affected by changes in pH.

The ESI-MS data confirm that the evolution with time of the initial species formed is strongly dependent on the amount of Pb(II) added and that over long time periods, the evolution leads to ESI-MS

detected species with lower Pb(II) content than the initial ones, as already observed in the case of the MT1 isoform and its individual domains [44]. The observed evolution and release of Pb(II) was clearly more remarkable in the case of the fragments than in the entire MT3, which maintains some of the highly Pb-loaded species even after 12 hours. These results suggest that a secondary process takes place, which promotes the release of Pb(II) ions from MT, or alternatively the formation of species no longer apparent by ESI-MS. But it is important to note that Pb(II) remains bound to MT3 for several hours and promotes the release of Zn^{2+} ions, which could, at least transiently, detoxify Pb(II) in the brain after exposure to this metal. The persistence of Pb_9- and Pb_{10}-MT3, even in the presence of low amounts of Pb(II), indicates that these species may play a special role in the Pb(II) binding.

Overall, these results indicate that the α and β domains of the mammalian MT3 isoform bind Pb(II) ions in a way that depends on the integrity of the entire protein. Both MT3 domains in the intact protein, can bind and retain Pb(II) after displacing Zn^{2+}, and Pb(II) remains bound for a long period of time whereas the separated fragments require a greater concentration of Pb(II) to displace all the Zn^{2+} initially bound, and the species formed disappear with time. Consequently, the data here presented allows to conclude that Pb(II) coordination to the entire MT3 is more favored than to its separated fragments. Interestingly, the equilibrium constants for the replacement of Zn(II) by Pb(II) in reactions with Zn-MT3, Zn-αMT3 and Zn-βMT3, as measured by ITC, are all similar. This suggest that, even if the stability of the Pb-species seems to be higher in the entire MT3 than in the isolated domains, probably the differences on stability between the Pb-MT formed and the initial Zn-MT species are very similar among the 3 peptides studied.

Conflicts of interest

There are no conflicts to declare.

Acknowledgements

The authors want to acknowledge Natacha Gilet who carried out some of the experiments here included during her short stay in our lab, and Ester Artells who carried out the clonation of the proteins here used. Authors from UAB are recipients of a MINECO-FEDER grant (BIO2015-67358-C2-2-P to MC) and members of the 2017SGR-864 Grup de Recerca de la Generalitat de Catalunya. Support from NSF grant CHE1710176 (RNA) is acknowledged. Finally, we want to express our gratitude to Silvia for having been with us for so many years, for having transmitted to us her energy and passion for science and for so many projects and shared dreams. You will always be an example to follow and in our most precious memories.

References

1. P. Grandjean, *Environ. Res.,* 1978, **17**, 303.
2. L. Patrick, *Alternative medicine review: a journal of clinical therapeutic,* 2006, **11**, 2.
3. I. Lehmann, U. Sack and J. Lehmann, 2011, 8, 157. *Metal Ions Affecting the Immune System*. In: *Metal Ions in Life Sciences*. Editors: A. Sigel, H. Sigel and R. K. O. Sigel.
4. H. R. Pohl, N. Roney, H. G. Abadin, Metal Ions Affecting the neurological System. In *Metal Ions in Life Sciences; Sigel, A.; Sigel, H. and Sigel, R.K.O.* Ed.; RSC Publishing: Cambridge, 2011, Vol 8, Chapter 10; pp 247-262.
5. J. Xu, H. C. Yan, B. Yang, L. S. Tong, Y. X. Zou and Y. Tian, *Journal of negative results in biomedicine,* 2009, **8**, 5.
6. T. E. Kober and G. P. Cooper, *Nature,* 1976, **262**, 704.
7. M. F. M. Braga, E. F. R. Pereira and E. X. Albuquerque, *Brain Res.,* 1999, **826**, 22.
8. L. D. White, D. A. Cory-Slechta, M. E. Gilbert, E. Tiffany-Castiglioni, N. H. Zawia, M. Virgolini, A. Rossi-George, S. M. Lasley, Y. C. Qian and M. Riyaz Basha, *Toxicol. Appl. Pharmacol.,* 2007, **225**, 1.
9. K. M. Bakulski, L. S. Rozek, D. C. Dolinoy, H. L. Paulson and H. Hu, *Curr. Alzheimer Res.*, 2012, **9**, 563.
10. J. Lee and J. L. Freeman, *NeuroToxicology*, 2014, **43**, 57.
11. S. Coon, A. Stark, E. Peterson, A. Gloi, G. Kortsha, J. Pounds, D. Chettle and J. Gorell, *Environ. Health Perspect.*, 2006, **114**, 1872.
12. J. M. Ordemann and R. N. Austin, *Metallomics*, 2016, **8**, 579.
13. A. Oskarssonl, K. S. Squibb and B. A. Fowler, *Biochem. Biophys. Res. Commun*., 1982, **104**, 290.
14. C. R. A. Santos, A. Martinho, T. Quintela and I. Gonçalves, *Life*, 2012, **64**, 126.
15. D. Juárez-Rebollar, C. Rios, C. Nava-Ruíz and M. Méndez-Armenta, *Oxid. Med. Cell Longev*., 2017, **2017**, 5828056.
16. K. T. Suzuki, N. Imura and M. Kimura, (Eds.), Metallothionein III, Birkhäuser Verlag, Basel, 1993.
17. C. D. Klaassen, (Ed.), Metallothionein IV, Birkhäuser Verlag, Basel, 1999.
18. Y. Uchida, K. Takio, K. Titani, Y. Ihara and M. Tomonaga, *Neuron,* 1991, **7**, 337.
19. G. Öz, K. Zangger and I. M. Armitage, *Biochem*., 2001, **40**, 11433.
20. J. Bousleiman, A. Pinsky, S. Ki, A. Su, I. Morozova, S. Kalachikov, A. Wiqas, R. Silver, M. Sever and R. N. Austin, *Int J Mol Sci*., 2017, **18**, 1133.
21. M. Vašák and G. Meloni, 2009, **5**, 319. *Metallothionein-3, Zinc, and Copper in the Central Nervous System*. In: *Metal Ions in Life Sciences*. Editors: A. Sigel, H. Sigel and R. K. O. Sigel.
22. A. Muñoz, D. H. Petering and C. F. Shaw, *Inorg. Chem*., 2000, **39**, 6114.
23. M. Capdevila, R. Bofill, Ò. Palacios and S. Atrian. *Coordination Chemistry Reviews*, 2012, **256**, 46.

24. N. Romero-Isart and M. Vašák, *J. Inorg. Biochem.,* 2002, **88**, 388.
25. P. Palumaa, I. Tammiste, K. Kruusel, L. Kangur, H. Jörnvall and R. Sillard, *Biochim Biophys Acta*, 2005, **1747**, 205.
26. C. A. Blindauer*, Chem. Comm.*, 2015, **51**, 4544.
27. S. Toriumi, T. Saito, T. Hosokawa, Y. Takahashi, T. Numata and M. Kurasaki, *Basic Clin. Pharmacol. Toxicol.,* 2005, **96**, 295.
28. P. Palumaa, E. Eriste, O. Njunkova, L. Pokras, H. Jörnvall and R. Sillard, *Biochemistry*, 2002, **41**, 6158.
29. T. Kochańczyk , A. Drozd and A. Krężel, *Metallomics*, 2015, **7**, 244.
30. J. Habjanič, O. Zerbe and E. Freisinger, *Metallomics*, 2018, doi: 10.1039/C8MT00193F.
31. J. S. Scheller, G. W. Irvine and M. J. Stillman, *Dalton Trans*., 2018, 47, 3613.
32. E. Artells, O. Palacios, M. Capdevila and S. Atrian, *FEBS J.,* 2014, **281**, 1659.
33. P. Palumaa, I. Tammiste, K. Kruusel, L. Kangur, H. Jörnvall and R. Sillard, *Biochim. Biophys. Acta*, 2005, **1747**, 205.
34. T. B. J. Pinter, G. W. Irvine and M. J. Stillman, *Biochemistry*, 2015, **54**, 5006.
35. P. Faller and M. Vašák, *Biochemistry*, 1997, **36**, 13341.
36. D. W. Hasler, P. Faller and M. Vašák, *Biochemistry*, 1998, **37,** 14966.
37. H. Wang, Q. Zhang, B. Cai, H. Li, K. H. Sze, Z. X. Huang, H. M. Wu and H. Sun, *FEBS Letters*,2006, **580**, 795.
38. B. Roschitzki and M. Vašák, *Biochem*. 2003, **42**, 9822.
39. G. Meloni, P. Faller and M. Vašák, *J. Biol. Chem*., 2007, **282**, 16068.
40. D. H. Petering, S. Krezosky and N. M. Tabatabai, 2009, **5**, 353. *Metallothionein Toxicology: Metal Ion Trafficking and Cellular Protection.* In: *Metal Ions in Life Sciences.* Editors: A. Sigel, H. Sigel, R. K. O. Sigel.
41. M. J. Stillman, D. Thomas, C. Trevithick, X. Guo, M. Siu, J. Inorg. Biochem., 2000, **79***,* 11.
42. W. Bernhard, M. Good, M. Vašák, J. H. R. Kägi, *Inorg*. *Chim*. *Acta,* 1983, **79**, 154.
43. D. Chu, Y. Tang, Y. Huan, W. He, W. Cao, *Thermochim. Acta*, 2000, **352-353**, 205.
44. O. Palacios, A. Leiva-Presa, S. Atrian, R. Lobinski, *Talanta*, 2007, **72**, 480.
45. Y. He, M. Liu, N. Darabedian, Y. Liang, D. Wu, J. Xiang, F. Zhou, *Inorg. Chem.,* 2014, **53**, 2822.
46. D. L. Wong, M. E. Marrifiel-MacRae and M. J. Stillman, 2017, **17**, 241. *Lead(II) Binding in Metallothioneins*. In: *Metal Ions in Life Sciences*. Editors: A. Sigel, H. Sigel and R. K. O. Sigel.
47. M. C. Carpenter, A. Shami Shah, S. DeSilva, A. Gleaton, A. Su, B. Goundie, M. L. Croteau, M. J. Stevenson, D. E. Wilcox, R. N. Austin, *Metallomics*, 2016, **8**, 605.
48. R. M. Harrison and D. P. H. Laxen, *Nature*, 1980, **286**, 791.
49. Q. Liu, Y. Liu, *J Colloid Interface Sci.,* 2003, **268**, 266.
50. S. J. Lee, B-R. Seo and J.-Y. Koh, *Molecular Brain*, 2015, **8**, 84.
51. M. Vašák and G. Meloni, *Int. J. Mol. Sci.*, 2017, **18**, 1117.
52. A. Rahman, K. Khan and M. S. Rao, *Neurotoxicol.*, 2018, **65**, 135.
53. M. Capdevila, N. Cols, N. Romero-Isart, R. González-Duarte, S. Atrian and P. González-Duarte, *Cell. Mol. Life Sci.*, 1997, **53**, 681.
54. N. Cols, N. Romero-Isart, M. Capdevila, B. Oliva, P. Gonzàlez-Duarte, R. Gonzàlez-Duarte and S. Atrian, *J. Inorg. Biochem.,* 1997, **68**, 157.
55. H. WeiGuo, C. DeYing, Y. JingYue, Y. DanFeng and S. MeiCheng. *Chem. Res. Chinese Universities*, 1999, **02**.
56. W. Xin, R. Bingen. *Chinese J. Biochem. Molec. Biol.*, 1999, **02**.
57. D.W. Smith, *J. Chem. Educ.*, 1977, **54**, 540.
58. J. H. Kagi and A. Schaffer, *Biochemistry*, 1988, **27**, 8509.

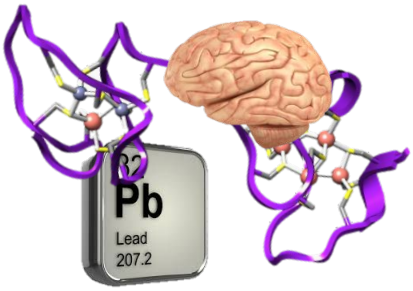

MT3 can bind Pb^{2+} to form a variety of metallated Pb-MT3 species